Meson-baryon dynamics in the nucleon-antinucleon system. II. Annihilation into two mesons

V. Mull, J. Haidenbauer, T. Hippchen, and K. Holinde
Institut für Kernphysik, Forschungszentrum Jülich, D-5170 Jülich, Germany
(Received 27 December 1990)

The annihilation of the nucleon-antinucleon ($N\bar{N}$) system into two mesons including π, η, η', ρ, ω, δ, a_1, a_2, f_2 as well as K and K^* is studied in a distorted-wave Born-approximation approach, in the conventional framework based on nucleon, delta-isobar, and hyperon (Λ, Σ, Y^*) exchange. Results for branching ratios are in fair agreement with the data; they show a strong sensitivity to the kind of initial-state interaction used. For polarizations and backward differential cross-section data of $p\bar{p} \to \pi^+\pi^-, K^+K^-$, there are characteristic discrepancies between experiment and model predictions; possible reasons are discussed.

I. INTRODUCTION

The annihilation of the $N\bar{N}$ system into several mesons is generally believed to be a good place for detecting explicit quark-gluon effects since relatively short interaction ranges are involved. In order to reach firm conclusions, however, it is of outstanding importance to reliably explore the limits of the conventional hadronic picture in describing annihilation phenomena. This in turn requires the use of a completely consistent description of all involved hadronic channels in order to possibly establish specific discrepancies with experimental data.

Within a conventional meson-theoretical approach annihilation proceeds via the exchange of baryons, the range of which is commonly related to their Compton wavelength of less than 0.2 fm. Since annihilation predominantly takes place at distances of nucleons and antinucleons around 1 fm, the conventional hadronic picture seems to be ruled out from the beginning and annihilation processes appear to be dominated by explicit quark-gluon dynamics. This conclusion, however, is not justified. We have shown recently [1] that baryon-exchange annihilation models, in spite of the small nucleon Compton wavelength, can indeed lead to an annihilation "range" around 1 fm. Thus, models based on baryon exchange still represent a valid alternative to currently more fashionable quark-gluon models.

From a theoretical point of view, annihilation into two mesons is of special interest since it is calculable in a relatively straightforward way. (A conventional calculation of annihilation into three or more mesons would be far more complicated.) In this work, we study the annihilation of the $N\bar{N}$ system into several two-meson channels including π, $\eta, \eta', \rho, \omega, \delta, a_1, f_2, a_2$ and the strange mesons K and K^* in a distorted-wave Born-approximation (DWBA) approach. Corresponding transition potentials are obtained from baryon-exchange diagrams involving not only nucleon-, but also delta (Δ)-isobar and hyperon (Λ, Σ, Y^*) exchange. As for the initial-state ($N\bar{N}$) interaction, we use various models developed by the same authors and described in the foregoing paper [2]. The elastic part has been taken to be the G-parity transform of the Bonn NN potential [3], using both the full interaction and the simple one-boson-exchange version (OBEPT). Two different approaches have been used to account for the annihilation. First, we have taken a simple phenomenological, complex, state- and energy-independent optical potential of Gaussian form; second, annihilation processes have been likewise derived in the meson-theoretical scheme, consisting of second iterations of effective transition interactions of the same type mentioned before. So far, we have neglected any final-state (meson-meson) interaction in our study, simply because not much is known about it at the relevant energies.

Anticipating our main results, we will show that our model is indeed able to reproduce the general trend of the existing annihilation data, although there are some discrepancies in the details. The latter, however, is not surprising since, among other possible reasons, the final-state interaction is not included. Nevertheless, the description is of the same quality as obtained from comparable calculations based on effective quark-gluon models [4]. A strong sensitivity of the results to the kind of initial-state interaction used has been observed.

In the next section, we describe our model for the $N\bar{N}$ annihilation processes in question. Section III contains a detailed presentation and discussion of the results. The paper ends with a short summary and outlook.

II. THE MODEL FOR $N\bar{N}$ ANNIHILATION

A. Basic features

In this work, we restrict ourselves to the study of those processes annihilating into two mesons only. Many (but not all) of these two-meson decay channels are empirically well established and provide already about 30% of the total annihilation. As mentioned before in the Introduction, we do not include effects of the final-state (meson-meson) interaction; apart from enlarging the complexity of the calculation, the main reason is that we do not know much about those forces, especially at the relevant energies. Indeed, as pointed out already by Green and Niskanen [4], a careful and consistent study of $N\bar{N}$ an-

nihilation channels might yield valuable information about these interactions.

In order to simplify matters further, we will assume in the following that the direct transition from the baryon-antibaryon to the meson sector occurs from the $N\bar{N}$ pair only. The annihilation amplitudes in channel space are then given by

$$\langle M_i M_j|T|N\bar{N}\rangle = \langle M_i M_j|V|N\bar{N}\rangle + \langle M_i M_j|V|N\bar{N}\rangle G_0(N\bar{N}) \times \langle N\bar{N}|T|N\bar{N}\rangle , \quad (2.1)$$

described pictorially in Fig. 1. Equation (2.1) reads more explicitly, in the c.m. system,

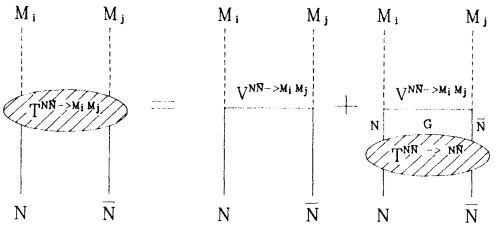

FIG. 1. Graphical representation of the DWBA approach to $N\bar{N}$ annihilation into two-meson channels.

$$\langle \mathbf{k}'\lambda_i'\lambda_j'|T(Z)|\mathbf{q}\lambda_N\lambda_{\bar{N}}\rangle = \langle \mathbf{k}'\lambda_i'\lambda_j'|V(Z)|\mathbf{q}\lambda_N\lambda_{\bar{N}}\rangle + \sum_{\lambda_N''\lambda_{\bar{N}}''} \int d^3q'' \langle \mathbf{k}'\lambda_i'\lambda_j'|V(Z)|\mathbf{q}''\lambda_N''\lambda_{\bar{N}}''\rangle \frac{1}{Z-2E_{q''}+i\varepsilon} \langle \mathbf{q}''\lambda_N''\lambda_{\bar{N}}''|T(Z)|\mathbf{q}\lambda_N\lambda_{\bar{N}}\rangle . \quad (2.2)$$

Here, $\mathbf{q}$, $\mathbf{q}''$, and $\mathbf{k}'$ are the initial, intermediate, and final relative momenta and λ_i the corresponding helicities. Z denotes the starting energy of the process.

Thus, in order to obtain the annihilation amplitude, we have to specify (i) the transition potential $\langle \mathbf{k}'\lambda_i'\lambda_j'|V(Z)|\mathbf{q}\lambda_N\lambda_{\bar{N}}\rangle$, (ii) the $N\bar{N}$ initial-state interaction $\langle \mathbf{q}''\lambda_N''\lambda_{\bar{N}}''|T(Z)|\mathbf{q}\lambda_N\lambda_{\bar{N}}\rangle$.

B. Transition potentials

Figure 2 shows the transition potentials which are needed in the following. For most processes, corresponding analytic expressions can be found in our foregoing paper, dealing with the $N\bar{N}$ interaction [2]. Additional expressions concerning the axial vector and tensor mesons are given in the Appendix.

The form factors have been parametrized in exactly the same way as for the elastic part of our initial-state interaction, i.e.,

$$F(\mathbf{p}_\delta) = \left[\frac{\Lambda_\alpha^2 - m_\delta^2}{\Lambda_\alpha^2 + \mathbf{p}_\delta^2}\right]^{n_\alpha} , \quad (2.3)$$

with $n_\alpha = 1$, apart from $n_\alpha = 2$ for the $N\Delta\rho$ and the NY^*K^* vertex. (Compared to the nucleon propagator, the propagator of a spin-$\frac{3}{2}$ particle involves higher powers of momenta; therefore, for the decuplet couplings involving vector mesons, $n_\alpha = 2$ is necessary in order to supply sufficient falloff at large momenta.) However, all Λ_α are treated as open parameters since the essential off-shell particle is now the exchanged baryon, not the meson as in the elastic part.

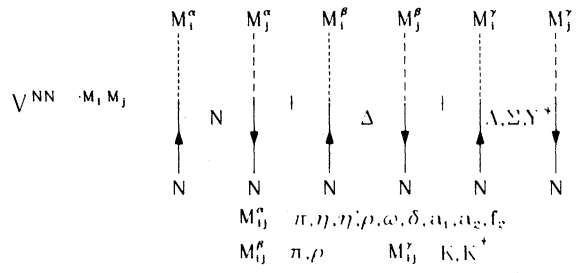

FIG. 2. Annihilation diagrams for the considered two-meson decay channels.

C. The initial-state interaction

In order to investigate the influence of the initial-state interaction on the results in specific annihilation channels we will use various $N\bar{N}$ interaction models, which are described extensively in the foregoing paper [2]. In model A, annihilation is parametrized by a phenomenological, state- and energy-independent optical potential. A(BOX) and A(OBE) differ in the elastic part: Starting point for A(BOX) is the (slightly modified) full Bonn NN potential whereas A(OBE) is based on a simple OBE version, both published in Ref. [3].

In model C, the annihilation part consists of second iterations of transition interactions based also on baryon exchange. Specifically, model C includes any combination of two mesons ($\pi,\rho,\omega,\delta,\sigma'$ and K,K^*), which is the same set as used in the elastic part. Note, that the σ' (with a mass of 550 MeV) is not a real particle but represents a simple effective description of correlated 2π

exchange processes. Therefore, the inclusion of σ' means that model C contains also some contribution due to three-meson annihilation (which is about 10%).

As we will see below, the explicitly treated two-meson annihilation channels account only for about 20% of the total annihilation. The remaining piece originates from decays into higher-mass mesons (e.g., f_2, a_2) and further contributions due to 3(4,5,. . .)-meson annihilation. Of course, a minimum requirement for a realistic initial-state interaction is that it at least roughly reproduces the total empirical annihilation. Since, at the present stage, it is impossible to explicitly calculate all missing contributions, we suitably increased the contributions so far included in our model, i.e., the channels not treated explicitly have been parametrized into those included. (This has been done essentially by using another type of form factor, see Ref. [2].) Therefore, the microscopic description of annihilation is still inconsistent and to a good part phenomenological: Although based on the same type of baryon-exchange diagrams, the annihilation processes in the initial-state interaction are considerably larger than in the actual transition.

In a certain sense, models A and C represent two extremes with the truth lying somewhere in between: In model C, the whole annihilation is parametrized using the strong spin, isospin, as well as energy dependence predicted by two-meson annihilation whereas those dependencies are totally suppressed in model A.

We stress that in the following calculations no parameter readjustment has been made in these initial-state interactions.

III. RESULTS AND DISCUSSION

There are two different types of experiments by which the annihilation of the $N\bar{N}$ system can be investigated. On one hand, one can measure branching ratios of decays into many different two-meson channels, starting from the protonium atom at rest. On the other hand, annihilation in flight can be studied in order to determine the energy dependence of various annihilation processes.

A. Annihilation at rest

The branching ratio B_{ij} is defined as the ratio of the partial width for the decay into mesons i and j vs the total annihilation width

$$B_{ij}=\frac{\Gamma_{ij}}{\Gamma_{\text{tot}}} . \tag{3.1}$$

Here, the partial width is obtained from

$$\Gamma_{ij}=\sum_{\lambda_i\lambda_j} 2\pi kE \int d\Omega_k |\langle \mathbf{k}\lambda_i\lambda_j | V | \Psi_{N\bar{N}} \rangle|^2 , \tag{3.2}$$

E being the total c.m. energy. Γ_{tot} is given by the sum of all partial widths.

Since we neglect the Coulomb interaction throughout this work, we replace in our theoretical calculations the protonium wave function by a scattering state of low energy ($E_{\text{lab}}=5$ MeV) and determine the branching ratio as a relative cross section. The same procedure has been used in other theoretical investigations too [5,6], suggested by experimental findings that relative cross sections at low energy and corresponding branching ratios at rest roughly agree for the $\pi^+\pi^-$ and K^+K^- channels [7]. Furthermore, model calculations [8] have shown that the difference is of the order of 20% only.

Quantum numbers and relevant properties of the mesons considered in this work are given in Table I. There are some meson combinations (e.g., $f_2\rho, f_2\omega, \ldots$) where the sum of the masses is larger than twice the nucleon mass, but still, due to their large width, the $N\bar{N}$ system can decay into those channels also at rest. Therefore, in such cases the meson widths cannot be neglected in the computation of the corresponding branching ratios. We assume a (normalized) mean distribution with a Breit-Wigner profile, neglecting any momentum dependence,

$$D_i(m_i)=\frac{1}{N_i}\frac{\Gamma_i^2}{4(m_{0,i}-m_i)^2+\Gamma_i^2} , \tag{3.3}$$

TABLE I. Masses, widths, and quantum numbers of the mesons included in our study.

		m (MeV/c^2)	Γ (MeV/c^2)	J^P	I^G
Pseudoscalar	π	138.03	0	0^-	1^-
	η	548.8	0	0^-	0^+
	η'	957.57	0	0^-	0^+
	K	495.82	0	0^-	$\frac{1}{2}$
	$\bar{K}$	495.82	0	0^-	$\frac{1}{2}$
Scalar	δ	983.0	54.0	0^+	1^-
Vector	ρ	782.6	155.0	1^-	1^+
	ω	769.0	10.0	1^-	0^-
	K^*	895.0	0	1^-	$\frac{1}{2}$
	$\bar{K}^*$	895.0	0	1^-	$\frac{1}{2}$
Axial vector	a_1	1100.0	316.0	1^+	1^-
Tensor	f_2	1270.0	180.0	2^+	0^+
	a_2	1350.0	110.0	2^+	1^-

with $N_i = \int dm_i D_i(m_i)$ and $m_{0,i}$, Γ_i the empirical mass and width of the meson. The observables are then evaluated by averaging over these distributions, e.g., the differential cross section is given by

$$\frac{\overline{d\sigma}}{d\Omega} = \int dm_1 dm_2 \frac{d\sigma}{d\Omega}(m_1,m_2) D_1(m_1) D_2(m_2) \times \Theta(2M_N - m_1 - m_2) \ . \quad (3.4)$$

1. *Branching ratios*

In this subsection we compare branching ratios obtained from $p\bar{p}$ annihilation at rest in liquid hydrogen with theoretically determined relative cross sections at low energy. It is known [4,9] that annihilation in liquid occurs by about 90% from S states and by 10% from states with higher angular momentum. Note that the dominant part of the cross section at low energies is given likewise by S-wave contributions. The total annihilation cross section at the considered laboratory energy of 5 MeV is assumed to be 427 mb, a value taken from an empirical parametrization of the cross section [10].

Those branching ratios for which experimental information is available are utilized to roughly fix the open parameters of our model—the cutoff masses appearing in the form factors of the transition potentials [see Eq. (2.3)]. They have been varied in steps of 100 (50) MeV; a more precise determination would improve the fit only marginally. The obtained values are given in Table II; they are the same for both initial-state interactions A(BOX) and A(OBE) but differ slightly for model C. We stress once more that these cutoff masses characterize essentially the off-shell behavior of the exchanged baryon and are therefore in principle different from those used at the corresponding vertices in the elastic $N\bar{N}$ interaction. It turns out, however, that they are in a comparable range (between 1 and 2 GeV). For completeness reasons, the coupling constants at the vertices of the transition potentials are also included in Table II. Most of these coupling constants are predetermined and taken from Table 9 in Ref. [3] or Table 7.2 of Ref. [11] while the remaining values are taken from Dumbrais *et al.* [12].

TABLE II. Coupling constants and cutoff masses used in the transition potentials pertaining to our models A and C. The underlined coupling constants are taken from the Bonn NN model (Ref. [3]) and its extension to the hyperon-nucleon case (Ref. [11]), respectively.

Vertex	g_i resp. $\hat{f}_i$	f_i/g_i	Λ_α A	C
$NN\pi$	0.2789		1500	1700
$N\Delta\pi$	0.4733		1600	1700
$NN\eta$	0.6535		1700	2000
$NN\eta'$	1.0493		1700	2000
$NN\delta$	1.6326		2500	2500
$NN\rho$	0.9165	6.1	1350	1850
$N\Delta\rho$	4.5222		1600	1800
$NN\omega$	4.4721	0	1500	1750
NNa_1	2.7019		2000	1500
NNf_2	2.0		2000	2000
NNa_2	2.0		2000	2000
$N\Lambda K$	−0.952		2000	2500
$N\Sigma K$	0.177		2000	2500
NY^*K	−0.193		2000	2500
$N\Lambda K^*$	−1.588	3.2588	1400	1400
$N\Sigma K^*$	−0.917	−2.4198	2200	2200
NY^*K^*	−1.846	0	2200	2200

The results of our calculations employing the different initial-state interactions introduced in the foregoing section are given in Table III. A first inspection shows a rough agreement with the data; it also reveals that there are remarkable discrepancies between the results using different initial-state interactions.

The largest contributions are provided by channels involving two vector mesons, in agreement with experiment. This follows automatically from the structure of the baryon-exchange model and is not a consequence of a specific choice of parameter values. Charged pions can be easily detected, so that the experimentally best known channel is the annihilation into a $\pi^+\pi^-$ pair although this branching ratio is comparatively small. In our model this annihilation process can proceed via exchange of a nucleon or a Δ isobar. Thus, we have two free parameters, namely, the cutoff masses at the $NN\pi$ and the $N\Delta\pi$ vertex. Their relative ratio, however, is constrained by additional observables (e.g., differential cross sections for annihilation in flight, to be discussed below) so that the relevant parameters are completely fixed by adjusting the strength in the $\pi^+\pi^-$ channel. Isospin relations then determine the results in the $\pi^0\pi^0$ channel.

ρ mesons are likewise generated by nucleon and Δ exchange. According to our calculations, the $\rho^+\rho^-$ channel yields a very large contribution to the total annihilation (up to 8%); other model calculations show the same trend. Unfortunately the corresponding branching ratio is not known experimentally since its determination requires the kinematical analysis of two neutral pions. The given upper limit of 9.5% corresponds to the value for the $\pi^+\pi^-\pi^0\pi^0$ channel, to which also the $\rho^+\rho^-$ pair contributes. Therefore, the two ρ-cutoff parameters have been mainly determined by the known branching ratios in the $\rho^0\rho^0$ and in the $\pi\rho$ channels. (Again, as in the $\pi\pi$ case, there are constraints due to annihilation in flight data.) Since the variation of each parameter has a similar effect, a good description of both channels is not possible. If, e.g., the parameter values are adjusted to reproduce the $\pi\rho$ channels, the branching ratio for $\rho^0\rho^0$ is much too large. Our final choice underestimates the $\pi^\pm\rho^\mp$ and the $\pi^0\rho^0$ channel and slightly overestimates the result in the $\rho^0\rho^0$ channel.

The ω-meson can be generated by nucleon exchange only. The corresponding cutoff parameter is fixed by the $\omega\omega$ channel. The results for the other channels involving the ω are then predetermined. The branching ratios for channels involving the η or η' are quite small, in agreement with experiment.

Experimental information involving scalar or tensor mesons is very limited. In addition, there are relatively large uncertainties in the corresponding coupling con-

stants. As a consequence cutoff masses cannot be determined uniquely and have been commonly fixed to 2 GeV. Whereas our results either agree or even exceed the experimental values for $f_2\pi^0$ and $a_2^{\pm}\pi^{\mp}$, the results for $f_2\rho^0$ and $f_2\omega$ are much too small. Thus the overall situation cannot be essentially improved by a change in the f_2 parameters. At this point one might ask the question whether the adjustment of form factors gives enough variation; in other words, whether a better fit can be obtained by varying some badly known coupling constants not fixed by NN scattering. This is not the case, for two reasons: First, due to their rather short range, baryon-exchange models are quite sensitive to the variation of form factor parameters; second, variation of coupling constants, e.g., f_2NN (like cutoff masses), changes the overall strength of the relevant channels ($f_2\pi, f_2\rho^0, f_2\omega$) but does not remove the deficiencies in the ratios between them.

In principle, of course, adjustments of coupling constants provide larger possibilities for variation since a contribution cannot be arbitrarily increased when using a form factor of type Eq. (2.3). Namely, there is a saturating effect when the cutoff mass is large enough ($\Lambda \gtrsim 2.5$ GeV). In almost all cases, however, this restricted range of variation was sufficient. An exception is the $\pi\delta$ channel: Our present result can only be brought into agreement with experiment by appreciably increasing (about a factor of 3) the δNN coupling constant, which is not known to a very good accuracy from NN scattering. However, the situation might well be different if a final-state $\pi\pi$ interaction is included: It probably modifies considerably the required pion cutoff masses ($\pi NN, \pi N\Delta$), which, in turn, leads to a completely different $\pi\delta$ branching ratio.

The strange mesons K and K^* are in our model mainly generated by Λ exchange, although Σ and Y^* exchange also contribute. The cutoff mass at the $N\Lambda K$ vertex has been fixed by the K^+K^- channel, the $N\Lambda K^*$ cutoff mass by $K^{*\pm}K^{\mp}$. Due to the insensitivity against variation of cutoff masses belonging to Σ and Y^*, the results for the other strange channels are then essentially predetermined.

Obviously, the trend of the data can be qualitatively reproduced. We stress that the present failure to reproduce quantitatively the ratios between all channels does not necessarily rule out the baryon-exchange concept. To our feeling, it rather points to the necessity of including realistic final-state interactions, which, as the initial-state interaction (see the discussion below), will surely change the results (even ratios) considerably. Alternatively, in

TABLE III. Branching ratios: Results obtained with our models in comparison with experimental data from annihilation at rest in liquid hydrogen (Refs. [9,29–35], compiled in Ref. [36]).

Channel	Branching ratios (%)			
$p\bar{p}\rightarrow$	A(OBE)	A(BOX)	C	Expt.
$\pi^+\pi^-$	0.43	0.39	0.58	0.33±0.017
$\pi^0\pi^0$	0.078	0.096	0.009	0.02–06
$\pi^0\eta$	0.014	0.014	0.000 84	0.03±0.02
$\eta\eta$	0.017	0.015	0.000 24	0.008±0.003
$\pi^0\eta'$	0.014	0.014	0.0025	0.05±0.02
$\eta\eta'$	0.031	0.042	0.0021	<0.018
$\rho^{\pm}\pi^{\mp}$	0.89	1.09	1.33	1.7±0.1
$\rho^0\pi^0$	0.50	0.58	1.11	1.4±0.1
$\rho^0\eta$	0.46	0.64	0.14	0.65±0.14
$\rho^0\eta'$	0.32	0.37	0.34	0.16±0.08
$\omega\pi^0$	1.48	2.18	0.070	0.52±0.05
$\omega\eta$	0.10	0.13	0.56	0.46±0.14
$\rho^+\rho^0$	5.24	7.41	5.63	(<9.5)
$\rho^0\rho^0$	0.91	1.07	0.14	0.4±0.3
$\rho^0\omega$	1.99	2.77	7.47	3.9±0.6
$\omega\omega$	1.29	1.66	0.50	1.4±0.6
$\pi^{\pm}\delta^{\mp}$	0.048	0.049	0.010	0.69±0.12
$f_2\pi^0$	0.41	0.65	3.26	0.41±0.12
$f_2\rho^0$	0.069	0.093	0.20	1.57±0.34
$f_2\omega$	0.31	0.25	0.068	3.05±0.31
$a_2^{\pm}\pi^{\mp}$	1.23	1.43	0.77	1.3–2.6
K^+K^-	0.13	0.21	0.072	0.1±0.01
$K^0\bar{K}^0$	0.038	0.062	0.1	0.08±0.01
$K^{\pm}K^{*\mp}$	0.13	0.12	0.019	0.1±0.016
$K^0\bar{K}^{*0}/K^{*0}K^0$	0.006	0.017	0.017	0.12±0.02
$K^{*+}K^{*-}$	0.061	0.094	0.075	0.13±0.05
$K^{*0}\bar{K}^{*0}$	0.019	0.029	0.070	0.26±0.05
Σ	18.52	24.18	24.69	30.94±3.91

view of the rather poor knowledge about meson-meson interactions in the relevant energy range, these data can hopefully be used to learn something about specific meson-meson interactions.

Table IV comprises our results for those channels in which there is at present no empirical information. Since almost all parameters have been fixed before, the numbers are essentially predictions. The contributions from channels involving the a_1 are very large; however, there are uncertainties in the corresponding coupling constant and, of course, in the cutoff parameter so that an experimental determination of branching ratios involving the a_1 would be very helpful. Nevertheless, our results suggest that such channels might bring up the contributions of the (empirically determined) two-meson decay modes of the protonium to about 50%, in comparison to about 30% at present.

We have already seen from Table III that the predicted branching ratios depend strongly on the kind of initial-state interaction used. In particular, the discrepancies between models A(BOX) and C, differing in the description of annihilation, are rather striking. We want to demonstrate this more clearly by using identical transition potentials (without parameter readjustment) for both initial-state interactions A(BOX) and C. Corresponding calculations are presented in Table V; they are performed with those parameter values in the transition potentials pertinent to model A(BOX). Therefore, the branching ratios for A(BOX) are the same as before whereas the values for model C do not coincide anymore with those in Table III, due to some variations in the cutoff masses of the transition potentials. Evidently, there are drastic differences between the results obtained from these initial-state interactions, although they both fit the total and elastic $N\bar{N}$ cross section with the same quality. Similar findings have been reported by Maruyama *et al.* [13]. Of course, some sensitivity to the initial-state interaction was to be expected since the various annihilation channels are subject to strong selection rules and therefore determined by contributions from specific partial waves. Yet, such rather large discrepancies are perhaps somewhat surprising.

TABLE IV. Branching ratios: Predictions of our models for channels where no experimental information is available.

Channel	Branching ratios (%)		
$p\bar{p}\rightarrow$	A(OBE)	A(BOX)	C
$\omega\eta'$	0.12	0.11	0.44
$\pi^0\delta^0$	0.017	0.016	0.0017
$\eta\delta^0$	0.093	0.050	0.040
$\eta'\delta^0$	0.0047	0.0038	0.0076
$\rho^{\pm}\delta^{\mp}$	0.43	0.44	1.55
$\rho^0\delta^0$	0.15	0.14	0.71
$\omega\delta^0$	0.58	1.16	0.35
$a_1^{\pm}\pi^{\mp}$	0.83	1.20	0.98
$a_1^0\pi^0$	0.41	0.41	0.64
$a_1^0\eta$	0.061	0.064	0.049
$a_1^0\eta'$	0.012	0.012	0.010
$\rho^{\pm}a_1^{\mp}$	1.93	3.87	6.96
$\rho^0a_1^0$	1.40	2.74	4.11
ωa_1^0	2.64	5.08	5.13
$f_2\eta$	0.068	0.081	0.0046
$a_2^0\eta$	0.007	0.011	0.053
$a_2^0\pi^0$	0.50	0.61	0.053
$a_2^{\pm}\rho^{\mp}$	0.006	0.010	0.017
$a_2^0\rho^0$	0.003	0.005	0.011
Σ	12.46	21.53	30.62

In addition, one can find in Table V predictions using the Born approximation only, i.e., neglecting the initial-state interaction completely. [The parameters in the transition potentials are again the ones pertaining to model A(BOX).] As already known in the literature [14], these results are much too large; they by far exceed the unitarity limit (in our case by a factor of 14). Therefore, we have normalized the sum to the corresponding value of A(BOX). It turns out that even the ratios of different branching ratios are completely changed. This raises serious doubt on any conclusions drawn from estimates based on the Born approximation only.

At the end of this subsection, we want to compare some of our results with those from other models available in the literature. The calculations of Kohno and Weise [5], Henley, Oka, and Vergados [6], and Maruyama, Furui, and Fässler [15] are based on a quark-gluon model for the transition process, differing in the choice of diagrams (rearrangement, annihilation) and the kind of annihilation vertex ($^3S_1, ^3P_0$). Furthermore, these groups use different initial-state interactions, which, as we just have seen, can have a strong impact on the results. Note that the authors of Refs. [5] and [6] do not quote absolute values for the branching ratios, but relative numbers compared to the $\pi^+\pi^-$ channel. The numbers cited in Table VI are based on a $\pi^+\pi^-$ branching ratio of 0.4. Wherever a range of values is given it means that the authors considered the contributions of different annihilation diagrams separately.

Obviously, there are sizable discrepancies between different quark-model predictions. Apart from uncertainties in the initial-state interaction, these arise from the choice of diagrams and annihilation vertices, mentioned before. For those branching ratios in which a comparison is possible, our results show qualitative agreement. Thus, at present, the data do not rule out nor even favor either concept.

Table VI includes also predictions made by Vandermeulen [16], who parametrizes the total $N\bar{N}$ annihilation in terms of transitions into two-meson channels only. These transitions are described phenomenologically assuming dominance near threshold, i.e., annihilation into heavy mesons is favored.

2. *Branching ratios from definite states*

In the last years, ASTERIX experiments at LEAR [7,17,18] have measured some branching ratios from protonium P states. Knowing the results from the annihilation in liquid hydrogen, the pure S-wave contributions

TABLE V. Effects of the initial-state interaction: All branching ratios (BR) are calculated with the transition potentials pertaining to model *A*.

Channel $p\bar{p}\rightarrow$	Born appr.	Branching ratios (%) parameters of model A *A*(OBE)	*A*(BOX)	*C*	Expt. BR (%)
$\pi^+\pi^-$	0.06	0.43	0.39	0.21	0.33±0.017
$\pi^0\pi^0$	0.000 74	0.078	0.096	0.0065	0.02–0.06
$\pi^0\eta$	0.000 46	0.014	0.014	0.001	0.03±0.02
$\eta\eta$	0.000 12	0.017	0.015	0.0003	0.008±0.003
$\pi^0\eta'$	0.000 43	0.014	0.014	0.002	0.05±0.02
$\eta\eta'$	0.000 38	0.031	0.042	0.002	<0.018
$\rho^\pm\pi^\mp$	3.41	0.89	1.09	0.575	1.7±0.1
$\rho^0\pi^0$	1.20	0.50	0.58	0.43	1.4±0.1
$\rho^0\eta$	0.49	0.46	0.64	0.061	0.65±0.14
$\rho^0\eta'$	0.20	0.32	0.37	0.21	0.16±0.08
$\omega\pi^0$	1.37	1.48	2.18	0.055	0.52±0.05
$\omega\eta$	0.65	0.10	0.13	0.43	0.46±0.14
$\rho^+\rho^-$	6.40	5.24	7.41	1.44	(<9.5)
$\rho^0\rho^0$	0.67	0.91	1.07	0.077	0.4±0.3
$\rho^0\omega$	2.42	1.99	2.77	4.81	3.9±0.6
$\omega\omega$	0.75	1.29	1.66	0.39	1.4±0.6
$\pi^\pm\delta^\mp$	0.0014	0.048	0.049	0.010	0.69±0.12
$f_2\pi^0$	0.43	0.41	0.65	2.75	0.41±0.12
$f_2\rho^0$	0.086	0.069	0.093	0.20	1.57±0.34
$f_2\omega$	0.073	0.31	0.25	0.051	3.05–0.31
$a_2^\pm\pi^\mp$	0.96	1.23	1.43	0.80	1.3–2.6
K^+K^-	0.072	0.13	0.21	0.028	0.1±0.01
$K^0\bar{K}^0$	0.000 28	0.038	0.062	0.015	0.08±0.01
$K^\pm K^{*\mp}$	0.21	0.13	0.12	0.019	0.1±0.016
$K^0\bar{K}^{*0}/K^{*0}\bar{K}^0$	0.0016	0.006	0.017	0.017	0.12±0.02
$K^{*+}K^{*-}$	0.084	0.061	0.094	0.075	0.13±0.05
$K^{*0}\bar{K}^{*0}$	0.0043	0.019	0.029	0.070	0.26±0.05
Σ	(24.15)	18.50	24.15	24.69	30.94±3.91

TABLE VI. Branching ratios: Comparison of our results with other calculations (Refs. [5,6,15,16]) and experimental data (Refs. [9,29–35]) for selected annihilation channels.

Channel $p\bar{p}\rightarrow$	*A*(BOX)	Other models (%) KW Ref. [5]	HOV Ref. [6]	MFF Ref. [15]	Vanderm. Ref. [16]	Expt. BR (%)
$\pi^+\pi^-$	0.39	(0.4)	(0.4)	0.12	0.54	0.33±0.017
$\pi^0\pi^0$	0.096		<0.045			0.02–0.06
$\pi^0\eta$	0.014	0.9–7.0	0.000 13			0.03±0.02
$\eta\eta$	0.015		<0.01			0.008±0.003
$\rho^\pm\pi^\mp$	1.09	3.3–4.6	1.9–2.7	2.1	1.75	1.7±0.1
$\rho^0\pi^0$	0.58	2.8	1.5–2.3			1.4±0.1
$\omega\pi^0$	2.18		1.1–1.3	0.8		0.52±0.05
$\rho^0\eta$	0.74		0.02			0.65±0.14
$\omega\eta$	0.13		0.1–0.2			0.46±0.14
$\rho^+\rho^-$	7.41	3.1–7.8	3.6–12.	0.4		(<9.5)
$\rho^0\rho^0$	1.07	0.2–2.8	0.3–4.4			0.4±0.3
$\rho^0\omega$	2.77		2.2–9.6	2.3	8.6	3.9±0.6
$\omega\omega$	1.66		2.8–9.3	0.4		1.4±0.6
$\pi^\pm\delta^\mp$	0.049				1.2	0.69±0.12
$f_2\pi^0$	0.65			0.09		0.41±0.12
$a_2^\pm\pi^\mp$	1.43			0.4	6.0	1.3–2.6
K^+K^-	0.21	0.1–0.2			0.11	0.1±0.01
$K^\pm K^{*\mp}$	0.12	0.9–1.8			0.4	0.1±0.016

TABLE VII. Results for branching ratios out of specific states in comparison with some data from the ASTERIX experiment (Refs. [7,17]).

Channel	BR from S state (%)				BR from P state (%)			
$p\bar{p}\rightarrow$	A(OBE)	A(BOX)	C	Expt.	A(OBE)	A(BOX)	C	Expt.
$\pi^+\pi^-$	0.43	(0.32)	0.89	0.32±0.02	0.39	(0.48)	0.045	0.48±0.049
$\pi^0\pi^0$	–	–	–	–	0.20	0.24	0.022	0.24±0.025
$\pi^0\eta$	–	–	–		0.036	0.021	0.0021	
$\eta\eta$	–	–	–		0.042	0.023	0.0006	
$\rho^\pm\pi^\mp$	1.09	1.38	1.93	1.55±0.1	0.38	0.42	0.12	1.04±0.22
$\rho^0\pi^0$	0.68	0.80	1.64	1.55±0.1	0.058	0.049	0.023	0.31±0.06
$\omega\pi^0$	2.07	3.20	0.0021		0.21	0.24	0.16	
$\rho^0\eta$	0.64	0.92	0.20		0.040	0.035	0.050	
$\omega\eta$	0.066	0.11	0.81		0.10	0.087	0.052	
$\rho^+\rho^-$	5.07	6.95	4.03		0.88	1.18	1.00	
$\rho^0\rho^0$	1.18	1.36	0.026		0.18	0.21	0.12	
$\rho^0\omega$	2.06	3.24	10.93		1.51	1.69	1.43	
$\omega\omega$	0.97	1.10	0.0073		0.88	0.78	0.26	
$\pi^\pm\delta^\mp$	0.022	0.021	0.000 92		0.025	0.029	0.010	
$f_2\pi^0$	0.44	0.69	5.06	0.24±0.07	0.34	0.54	0.21	0.81±0.19
$f_2\rho^0$	0.11	0.14	0.32		0.0048	0.0062	0.0052	
$f_2\omega$	0.48	0.37	0.10		0.027	0.025	0.0089	
$a_2^\pm\pi^\mp$	1.76	2.00	0.47		0.32	0.44	0.22	
K^+K^-	0.16	0.12	0.11	0.11±0.01	0.066	0.047	0.0023	0.03±0.01
$K^0\bar{K}^0$	0.016	0.011	0.16	0.08±0.01	0.068	0.045	0.0012	0.01±0.002
$K^\pm K^{*\mp}$	0.10	0.14	0.026			0.015	0.0069	
$K^0\bar{K}^{*0}/K^{*0}\bar{K}^0$	0.009	0.017	0.027			0.0017	0.000 72	
$K^{*+}K^{*-}$	0.05	0.062	0.094		0.0059	0.015	0.0017	
$K^{*0}\bar{K}^{*0}$	0.014	0.019	0.068		0.0034	0.0060	0.000 47	

could then be determined as well.

Table VII contains the corresponding quantities calculated with our models. Since there is no experimental information on the magnitude of the total annihilation cross section out of pure S (P) waves, we fix them by requiring that the $\pi^+\pi^-$ branching ratio predicted by model A(BOX) agrees with the experimental values. All further results are then renormalized to these values.

Again, for both S and P states, we observe sizable differences between the model predictions. In those channels where data are available, our models roughly agree with the experimental values. (An exception is the $f_2\pi^0$ channel derived from model C.) Obviously, it would be important to have further empirical information, especially for those channels involving various combinations of vector mesons, which dominate the total annihilation.

3. *The "πρ puzzle" and related questions*

Already at the end of the 1960s, $\pi\rho$ branching ratios in liquid hydrogen have been determined [19]. Contrary to naive expectations, it has been found that the values are essentially the same for all charge combinations $\pi^\pm\rho^\mp, \pi^0\rho^0$. The $\pi^0\rho^0$ combination being a pure isospin-0 state can annihilate only from the $({}^3S_1, I=0)$ protonium state, whereas the charged combinations can also be generated from the $({}^1S_0, I=1)$ state. Since both S states in protonium should be populated with about the same probability, the annihilation from the ${}^1S_0$ state in the $\pi\rho$ channel is obviously strongly suppressed implying a dynamical selection rule [20]. First measurements at LEAR [21] investigating the annihilation from P states into the $\pi\rho$ channel indicated a similar suppression of the $I=1$ states also in P waves. New ASTERIX measurements [17], however, contradict these results.

Alternatively, one can study annihilation into different channels from the same initial state. Considering ratios of these channels, one might then hope to minimize the effect of the initial-state interaction [22]. Another interesting comparison is possible by looking at combinations (ratios) of channels with and without strangeness.

Some of those ratios are given in Table VIII. In clear contradiction to the aforementioned hopes and expectations, even these quantities depend considerably on the kind of initial-state interaction used. For $\pi\rho$ decays from S states, all models yield values smaller than one, although not as small as given by experiments. For P states, our predictions definitely favor the new ASTERIX data ruling out any "$\pi\rho$ puzzle" here.

B. Annihilation in flight

1. *Integrated cross section*

So far, the energy dependence of the annihilation has been determined for relatively few channels only. Corre-

TABLE VIII. "$\pi\rho$ puzzle" and various ratios as obtained with our models versus experimental information (Ref. [22]).

	Our results			
	A(OBE)	A(BOX)	C	Experiment
$\frac{p\bar{p}(^1S_0, I=1) w \to \rho^{\pm}\pi^{\mp}}{p\bar{p}(^3S_1, I=0) \to \rho^{\pm}\pi^{\mp}}$	0.61	0.73	0.18	0.07±0.03
$\frac{p\bar{p}(^3P_1, I=1) \to \rho^{\pm}\pi^{\mp}}{p\bar{p}(^1P_1, I=0) \to \rho^{\pm}\pi^{\mp}}$	1.58	2.64	2.83	1.33±0.7
$\frac{p\bar{p}(^3S_1, I=1) \to a_2^{\pm}\pi^{\mp}}{p\bar{p}(^1S_0, I=0) \to a_2^{\pm}\pi^{\mp}}$	1.51	1.35	13.88	0.13±0.03
$\frac{p\bar{p}(^3S_1, I=1) \to \rho^0\eta}{p\bar{p}(^3S_1, I=0) \to \omega\eta}$	9.76	9.19	0.25	0.55±0.12
$\frac{p\bar{p}(^3S_1, I=1) \to \rho^0\omega}{p\bar{p}(^1S_0, I=0) \to \omega\omega}$	2.13	3.1	1545.3	0.81±0.35
$\frac{p\bar{p}(^3S_1, I=1) \to f_2\rho^0}{p\bar{p}(^3S_1, I=1) \to f_2\omega}$	0.22	0.43	3.15	0.53±0.15
$\frac{p\bar{p}(^3S_1) \to K^+K^- + K^0\bar{K}^0}{p\bar{p}(^3S_1) \to \pi^+\pi^-}$	0.41	0.42	0.31	0.60±0.05
$\frac{p\bar{p}(^1S_0) \to K^{*\pm}K^{\mp} + K^{*0}\bar{K}^0}{p\bar{p}(^1S_0) \to \rho^{\pm}\pi^{\mp}}$	0.26	0.27	0.18	0.70±0.30
$\frac{p\bar{p}(^3P_{0/2}) \to K^+K^- + K^0\bar{K}^0}{p\bar{p}(^3P_{0/2}) \to \pi^+\pi^-}$	0.34	0.19	0.08	0.078±0.014

sponding model predictions are presented in Fig. 3, for channels involving pseudoscalar and vector mesons. Note that our calculations are restricted to laboratory momenta below 780 MeV/c. Above this energy free pions can be created (without $N\bar{N}$ annihilation) which is not taken into account by our model (nor in any other $N\bar{N}$ model we know of). In general, our results roughly reproduce the trend of the data. This is, however, not true for channels involving tensor mesons; see Fig. 4. As observed already for the branching ratios at rest, the $f_2\pi$ channel is considerably overestimated by our models whereas the opposite happens for the $f_2\rho$ channel. An essential improvement can probably only be reached by including a suitable final-state interaction.

2. *Differential cross sections*

For several years, angular distributions for the annihilation in flight are available for the $\pi^+\pi^-$ and K^+K^- channels [23,24]. Such angular dependent observables are determined by the relative strength of the partial-wave contributions and, for the particular case of annihilation into two pseudoscalar mesons, are sensitive to the properties of relatively few partial waves only.

In the $\pi^+\pi^-$ channel the differential cross sections resulting from the models A(OBE) and A(BOX) are rather similar (cf. Fig. 5); they roughly agree with the experiments in forward direction. There are, however, increasing shortcomings with higher energies; in particular, all our models do not reproduce the observed rise of the cross section in backward direction. Indeed, some models developed by other authors [14,25,26] do much better in this aspect. For example, Moussallam, who presented a comparable baryon-exchange model, can reproduce the data in this energy region quite well [14]. This is obviously due to a different treatment of the Δ-exchange part of his transition potential, leading to an enhancement in the contributions from the $J=2$ partial waves and subsequently to a reproduction of the backward peak.

The situation in the K^+K^- channel can be seen in Fig. 6. Also here, the data clearly show a rise in the backward region, in contrast to our model predictions. It should be mentioned, however, that other theoretical models

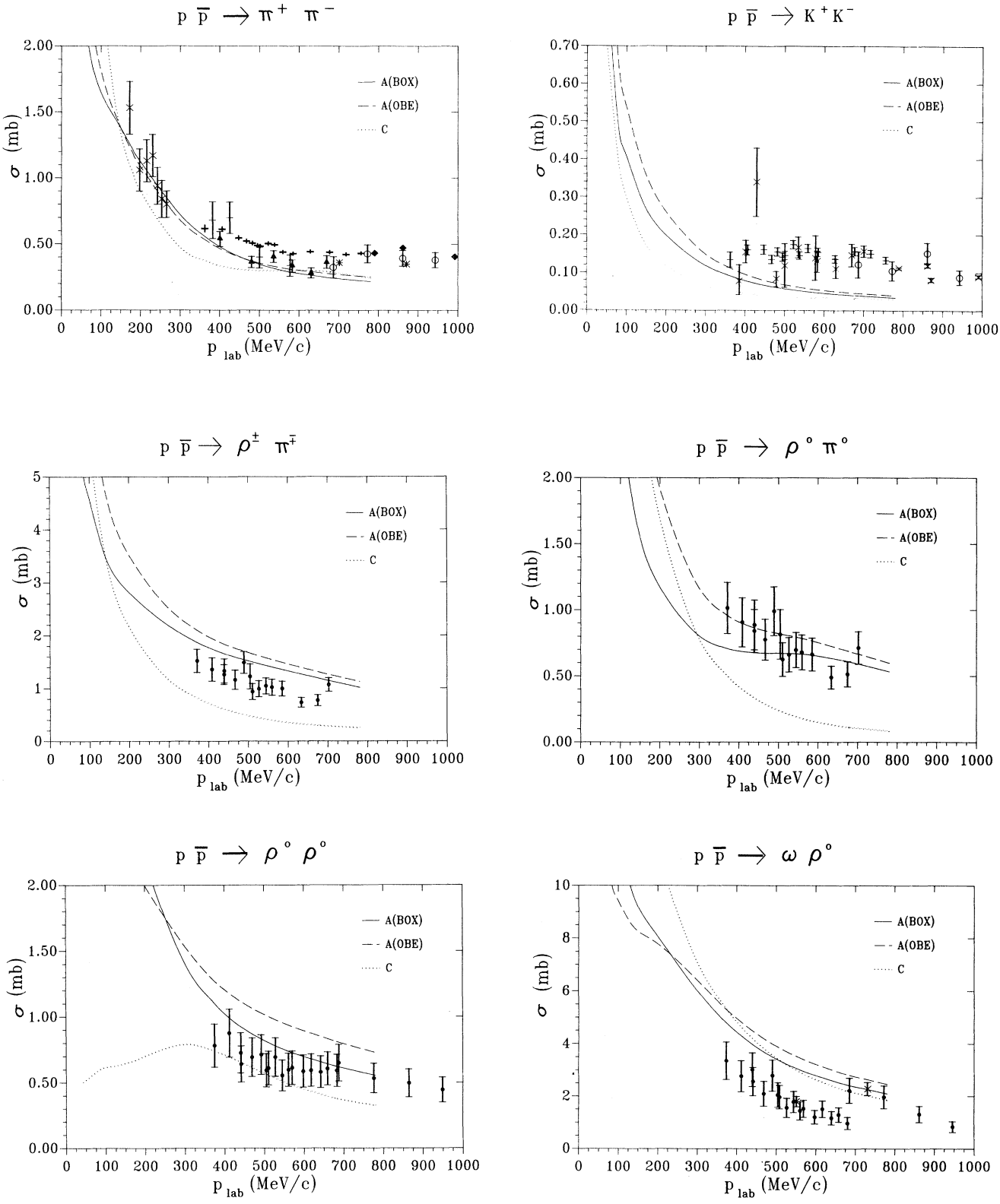

FIG. 3. Integrated cross sections for annihilation into channels with pseudoscalar or vector mesons obtained from our models A(OBE), A(BOX), and C. Experimental data for the $p\bar{p} \to \pi^+\pi^-$ and $p\bar{p} \to K^+K^-$ channels are taken from Refs. [23,24,37–41], those for the other channels from Refs. [37] and [42].

[25,26] have similar deficiencies for backward angles. Again, the consideration of final-state interactions together with transitions like $p\bar{p} \rightarrow \Lambda\bar{\Lambda} \rightarrow K\bar{K}$ (as emphasized in Ref. [27]) might improve the situation.

3. *Analyzing powers*

Recently, analyzing powers have been measured at LEAR [28] in the same channels, which are shown in Figs. 7 and 8. Again, the predictions for models A(OBE) and A(BOX) are quite similar whereas the results derived from model C differ drastically. None of the models is able to reproduce the data; especially model C shows a completely different behavior in the backward region.

IV. SUMMARY AND OUTLOOK

In this paper, we have studied the $N\bar{N}$ annihilation into two mesons, using a model based on baryon $(N, \Delta, \Lambda, \Sigma, Y^*)$ exchange. Most coupling constants and meson parameters have been taken over from previous studies in the nucleon-nucleon and hyperon-nucleon sector, carried out also by the Bonn-Jülich group [3,11]. For

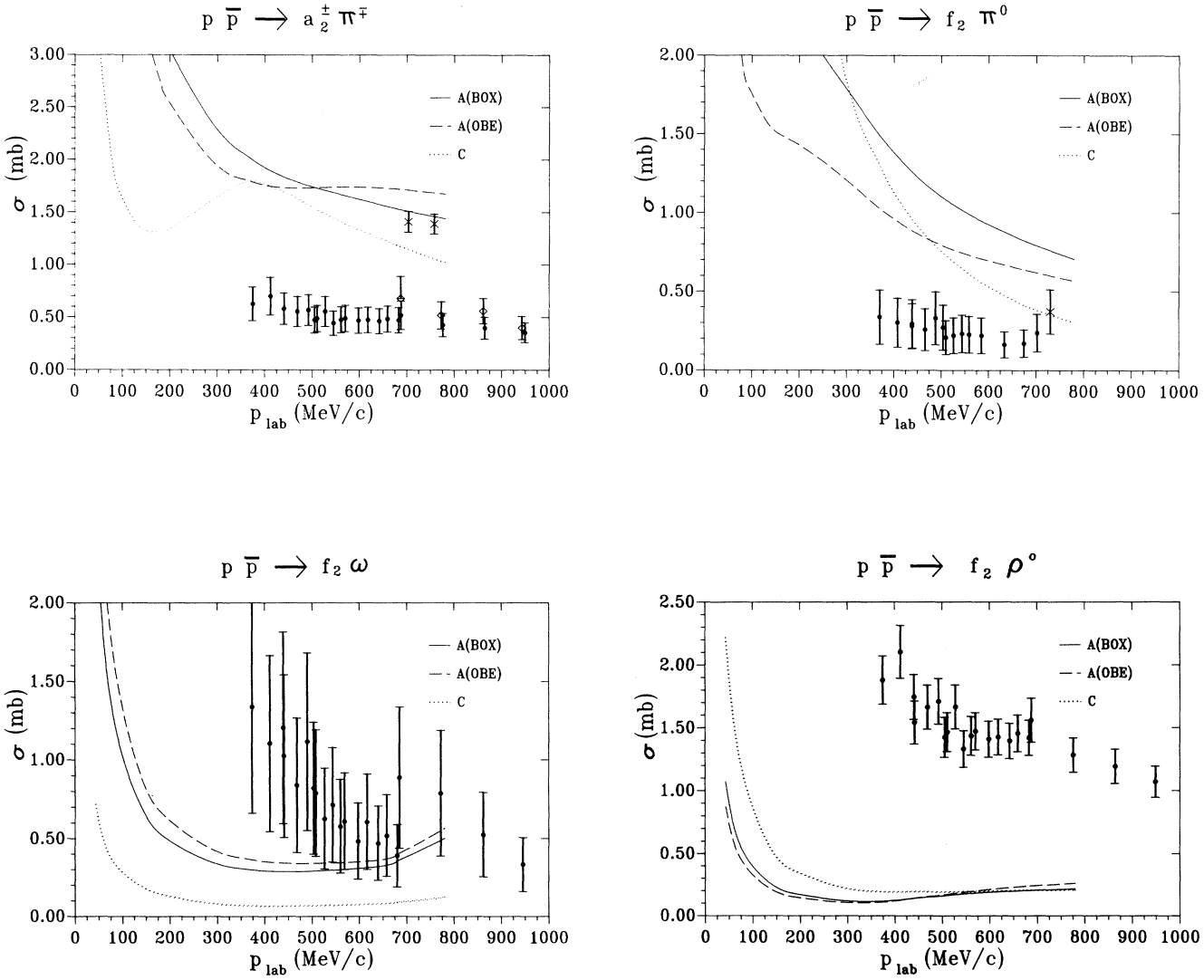

FIG. 4. Integrated cross sections for annihilation into channels with one tensor meson. Same description of the curves as in Fig. 3. Experimental data are taken from Refs. [37,43].

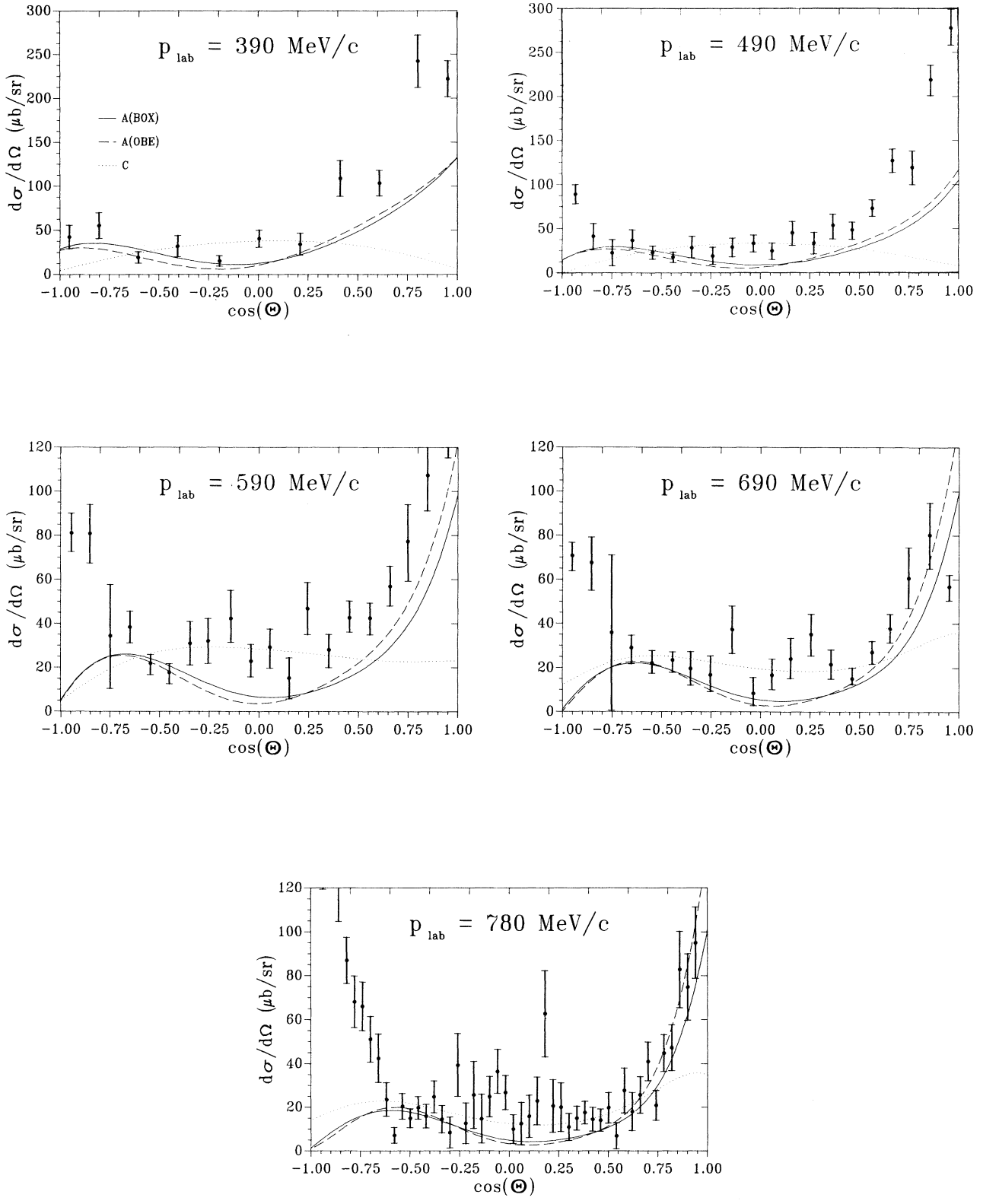

FIG. 5. Differential cross sections for the annihilation process $p\bar{p} \to \pi^+\pi^-$ at various energies. Same description of the curves as in Fig. 3. Experimental data are taken from Refs. [23,24].

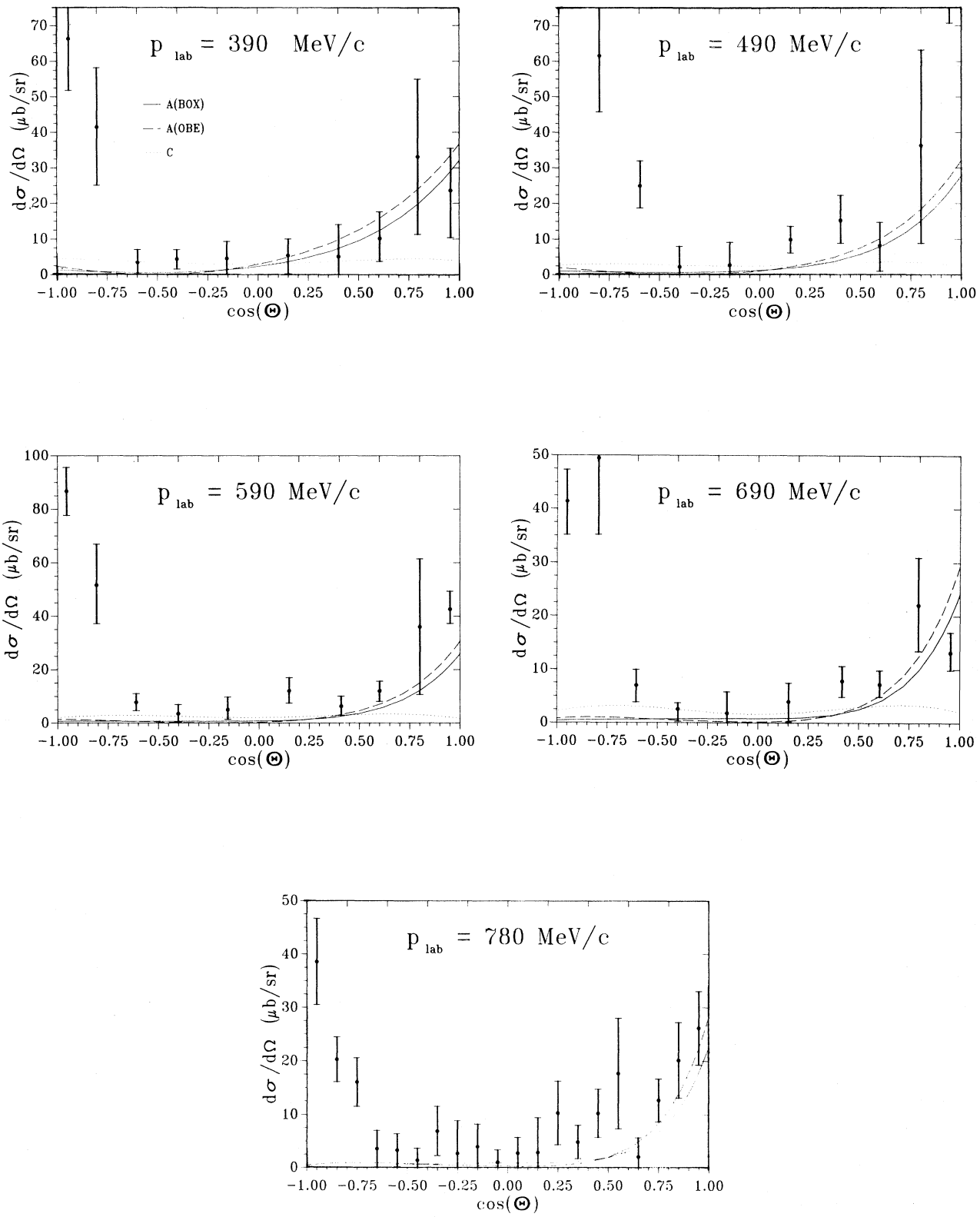

FIG. 6. Differential cross sections for the annihilation process $p\bar{p} \rightarrow K^+K^-$ at various energies. Same description of the curves as in Fig. 3. The experimental data are taken from Refs. [23,24].

the others, experimental information has been used. The cutoff masses, however, had to be treated as open parameters since the baryon, not the meson as before, is now the essential off-shell particle in the transition process.

We have used several initial-state $N\bar{N}$ interactions all based on the Bonn NN potential, which differ either in the elastic or in the annihilation part. The main outcome of our work is that essentially all results, even ratios of cross sections in different annihilation channels, depend sensitively on the kind of initial-state interaction used. In most cases, the trend of the data can be roughly reproduced; the description is of (at least) the same quality as obtained from comparable quark-gluon models. Thus, for the moment, there is absolutely no indication for the dominance or even relevance of explicit quark-gluon dynamics, in $N\bar{N}$ annihilation.

Severe discrepancies have been found at some places between our model predictions and existing data. In our opinion, these deficiencies indicate the need for an inclusion of realistic final-state effects, which have demonstrated already their outstanding role in the $p\bar{p}\to\Lambda\bar{\Lambda}$ process. Unless this is done, in consistency with the underlying scheme, it is certainly premature to draw any reliable conclusions on the success or failure of either the conventional baryon-exchange approach or treatments based on effective quark-gluon exchange models. Furthermore, in view of the established sensitivity to initial- (and possibly final-) state interactions employed, it seems also to be too early to discuss relative merits and shortcomings of different quark-gluon processes.

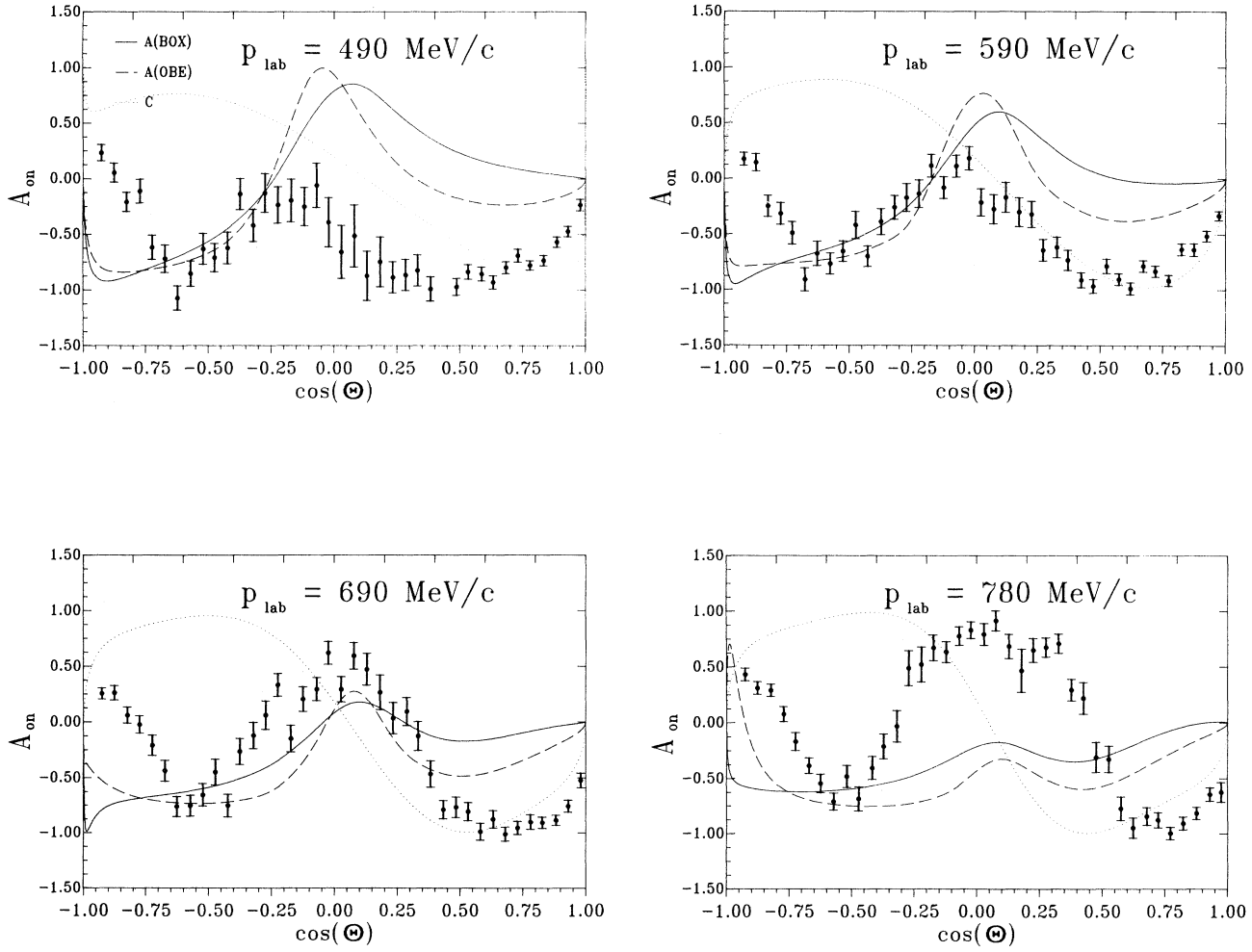

FIG. 7. Analyzing powers for the annihilation process $p\bar{p}\to\pi^+\pi^-$ at various energies. Same description of the curves as in Fig. 3. (Preliminary) Experimental data are taken from Ref. [28].

ACKNOWLEDGMENTS

Thanks are due to Professor J. Speth for his encouraging support and numerous enlightening discussions throughout the course of this work. We also thank Dr. B. Moussallam for providing us with his computation code, which enabled us to make a detailed comparison of the calculations.

APPENDIX: TRANSITION POTENTIALS INVOLVING a_1, a_2, AND f_2 MESONS

The starting point is the interaction Lagrangians specifying the coupling of the nucleon to the axial vector and tensor mesons,

axial vector meson 1^+:

$$\mathcal{L}_a = \sqrt{4\pi} g_a \bar{\Psi}_{N'}(x)\gamma^5\gamma^\mu \Psi_N(x)\Phi^j_\mu(x) , \tag{A1a}$$

tensor meson 2^+:

$$\mathcal{L}_t = \sqrt{4\pi}\frac{g_t}{m_N}\{i\bar{\Psi}_{N'}(x)[\gamma^\mu\partial^\nu\Psi_N(x)+\gamma^\nu\partial^\mu\Psi_N(x)] - i[\partial^\nu\bar{\Psi}_{N'}(x)\gamma^\mu+\partial^\mu\bar{\Psi}_{N'}(x)\gamma^\nu]\Psi_N(x)\} \times \Phi^j_{\mu\nu}(x) , \tag{A1b}$$

where Ψ_N denotes the nucleon field operator and Φ^j_μ ($\Phi^j_{\mu\nu}$) the corresponding operator for the axial vector (tensor) meson. Using the ansatz for the interaction

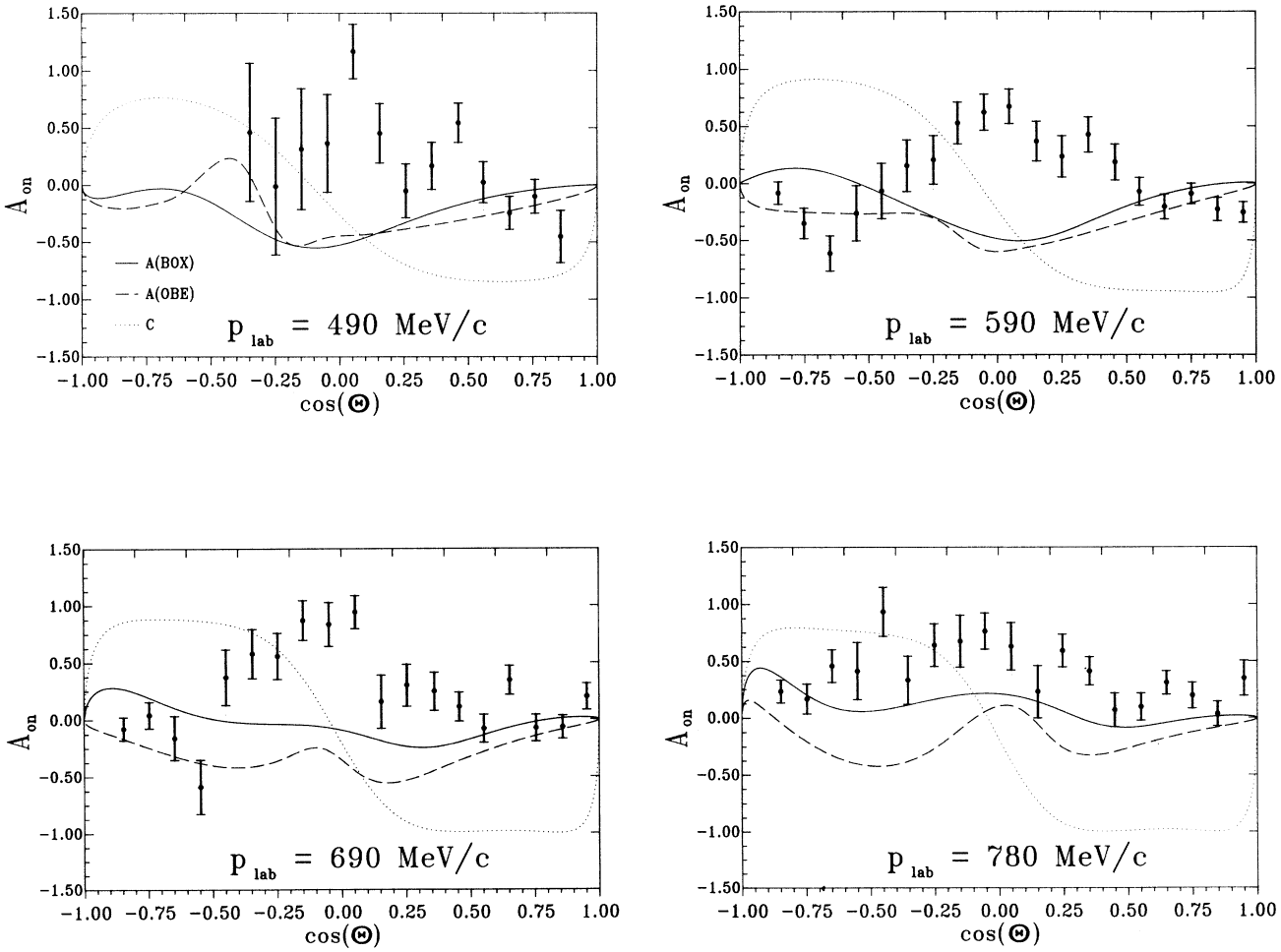

FIG. 8. Analyzing powers for the annihilation process $p\bar{p}\to K^+K^-$ at various energies. Same description of the curves as in Fig. 3. (Preliminary) Experimental data are taken from Ref. [28].

Hamiltonian

$$W=-\int d^3x\,\mathcal{L}\ , \tag{A2}$$

the corresponding transition potentials, being of second order in W,

$$\langle M_iM_j|V|N\bar{N}\rangle\equiv\left\langle M_iM_j\left|W\frac{1}{Z-H_0+i\varepsilon}W\right|N\bar{N}\right\rangle\ , \tag{A3}$$

can be evaluated in a straightforward way. The result can be split into four different contributions, namely, two time orderings together with exchange contributions; see Fig. 9. The latter can simply be taken into account by a factor of 2 in the allowed states. In the following, we give the result for the first time ordering only; the extension to the second one is obvious, see Ref. [2].

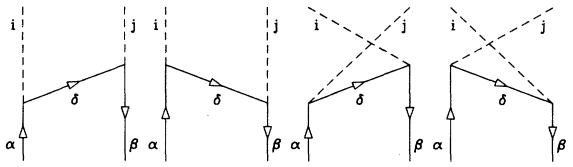

FIG. 9. Two time orderings of the transition potential and corresponding exchange diagrams.

The evaluation of Eq. (A3) yields the following results for an axial vector and a pseudoscalar meson:

$$\langle\mathbf{k}\lambda_i0|^1U_{ij}(Z)|\mathbf{q}\lambda_N\lambda_{\bar{N}}\rangle=\frac{f_i}{m_j}\frac{F^i(p_\delta^2)F^j(p_\delta^2)}{4\pi^2}\frac{1}{\sqrt{\omega_k^i\omega_k^j}(Z-\omega_k^i-E_\delta-E_N)}$$
$$\times\left[\bar{u}(\mathbf{q},\lambda_N)g_i\gamma^5\gamma^\mu\varepsilon_\mu(\mathbf{k},\lambda_i)\frac{1}{2E_\delta}(\gamma^0E_\delta-\boldsymbol{\gamma}\cdot\mathbf{p}_\delta+M_\delta I_4)\gamma^5\gamma^\tau k_\tau^j v(-\mathbf{q},\lambda_{\bar{N}})\right]^*\ , \tag{A4}$$

a vector and an axial vector meson:

$$\langle\mathbf{k}\lambda_i\lambda_j|^1U_{ij}(Z)|\mathbf{q}\lambda_N\lambda_{\bar{N}}\rangle=\frac{F^i(p_\delta^2)F^j(p_\delta^2)}{4\pi^2}\frac{1}{\sqrt{\omega_k^i\omega_k^j}(Z-\omega_k^i-E_\delta-E_N)}$$
$$\times\left[\bar{u}(\mathbf{q},\lambda_N)\left[g_i\gamma^\mu+i\frac{f_i}{2M_N}\sigma^{\mu\nu}k_\nu^i\right]\varepsilon_\mu(\mathbf{k},\lambda_i)\right.$$
$$\left.\times\frac{1}{2E_\delta}(\gamma^0E_\delta-\boldsymbol{\gamma}\cdot\mathbf{p}_\delta+M_\delta I_4)g_i\gamma^5\gamma^\tau\varepsilon_\mu(\mathbf{k},\lambda_i)v(-\mathbf{q},\lambda_{\bar{N}})\right]^*\ , \tag{A5}$$

a tensor and a pseudoscalar meson:

$$\langle\mathbf{k}\lambda_i0|^1U_{ij}(Z)|\mathbf{q}\lambda_N\lambda_{\bar{N}}\rangle=\frac{g_i}{M_N}\frac{f_j}{m_j}\frac{F^i(p_\delta^2)F^j(p_\delta^2)}{4\pi^2}\frac{1}{\sqrt{\omega_k^i\omega_k^j}(Z-\omega_k^i-E_\delta-E_N)}$$
$$\times\left\{\bar{u}(\mathbf{q},\lambda_N)[(q+p_\delta)^\nu\gamma^\mu+(q+p_\delta)^\mu\gamma^\nu]\varepsilon_{\mu\nu}(\mathbf{k},\lambda_i)\right.$$
$$\left.\times\frac{1}{2E_\delta}(\gamma^0E_\delta-\boldsymbol{\gamma}\cdot\mathbf{p}_\delta+M_\delta I_4)\gamma^5\gamma^\tau k_\tau^i v(-\mathbf{q},\lambda_{\bar{N}})\right\}^*\ , \tag{A6}$$

a tensor and a vector meson:

$$\langle\mathbf{k}\lambda_i\lambda_j|^1U_{ij}(Z)|\mathbf{q}\lambda_N\lambda_{\bar{N}}\rangle=\frac{g_i}{M_N}\frac{f_j}{m_j}\frac{F^i(p_\delta^2)F^j(p_\delta^2)}{4\pi^2}\frac{1}{\sqrt{\omega_k^i\omega_k^j}(Z-\omega_k^i-E_\delta-E_N)}$$
$$\times\left[\bar{u}(\mathbf{q},\lambda_N)[(q+p_\delta)^\nu\gamma^\mu+(q+p_\delta)^\mu\gamma^\nu]\varepsilon_{\mu\nu}(\mathbf{k},\lambda_i)\frac{1}{2E_\delta}(\gamma^0E_\delta-\boldsymbol{\gamma}\cdot\mathbf{p}_\delta+M_\delta I_4)\right.$$
$$\left.\times\left[g_j\gamma^\tau+i\frac{f_j}{2M_N}\sigma^{\tau\rho}k_\rho^j\right]\varepsilon_\tau(-\mathbf{k},\lambda_j)v(-\mathbf{q},\lambda_{\bar{N}})\right]^*\ . \tag{A7}$$

For the evaluation of the last potential (tensor-vector), the three-momentum of the exchanged nucleon, $\mathbf{p}_\delta$, has been neglected in the nucleon projection operator $\Lambda_\pm$. This simplifies the calculations enormously and seems to be justified since nucleon and meson masses are quite similar in this case, implying that the momentum transfer for the on-shell process is small.

The above expressions have to be multiplied by suitable isospin factors, which can be found in Table I of Ref. [2].

[1] J. Haidenbauer, T. Hippchen, K. Holinde, and J. Speth, Z. Phys. A **334**, 467 (1989); J. Haidenbauer, T. Hippchen, and K. Holinde, Nucl. Phys. **A508**, 329c (1990).
[2] T. Hippchen, J. Haidenbauer, K. Holinde, and V. Mull, Phys. Rev. C **44**, 1323 (1991), the preceding paper.
[3] R. Machleidt, K. Holinde, and Ch. Elster, Phys. Rep. **149**, 1 (1987).
[4] A. M. Green and J. A. Niskanen, in *Progress in Particle and Nuclear Physics, Vol. 18,* edited by A. Fässler (Pergamon, New York, 1987), p. 93.
[5] M. Kohno and W. Weise, Phys. Lett. **152B**, 303 (1985).
[6] E. M. Henley, T. Oka, and J. Vergados, Phys. Lett. **166B**, 274 (1986).
[7] R. Landua, Nucl. Phys. B (Proc. Suppl.) **8**, 179 (1989).
[8] J. Carbonell, G. Ihle, and M. Richard, Z. Phys. A **334**, 329 (1989).
[9] R. Armenteros and B. French, in *High Energy Physics IV,* edited by E. H. S. Burhop (Academic, New York, 1969).
[10] T. Brando *et al.,* Phys. Lett. **158B**, 505 (1985).
[11] B. Holzenkamp, K. Holinde, and J. Speth, Nucl. Phys. **A500**, 485 (1989).
[12] O. Dumbrais, R. Koch, H. Pilkuhn, G. C. Oades, H. Behrens, J. J. de Swart, and P. Kroll, Nucl. Phys. **B216**, 277 (1983).
[13] M. Maruyama, T. Gutsche, G. Strobel, A. Faessler, and E. M. Henley, Phys. Lett. B **215**, 223 (1988).
[14] B. Moussallam, Nucl. Phys. **A407**, 413 (1983); **A429**, 429 (1984).
[15] M. Maruyama, S. Furui, and A. Faessler, Nucl. Phys. **A472**, 643 (1987).
[16] J. Vandermeulen, Z. Phys. C **37**, 563 (1988).
[17] B. May *et al.,* Nucl. Phys. B (Proc. Suppl.) **8**, 218 (1989).
[18] M. Doser *et al.,* Nucl. Phys. **A486**, 493 (1988); Phys. Lett. B **215**, 792 (1988).
[19] M. Foster, P. Gavillet, G. Labrosse, L. Montanet, R. A. Salmeron, and P. Villemoes, Nucl. Phys. **B6**, 107 (1968).
[20] C. B. Dover, in *Windsurfing the Fermi Sea,* edited by T. T. S. Kuo and J. Speth (Elsevier Science, British Vancouver, 1987); C. B. Dover, P. M. Fishbane, and S. Furui, Phys. Rev. Lett. **57**, 1538 (1986).
[21] S. Ahmad *et al.,* in *Proceedings of the VII European Symposium on Antiproton Interactions, Durham, England, 1984,* edited by M. R. Pennington (Adam Hilger Ltd., Bristol, 1985), p. 287.
[22] E. Klempt, Z. Phys. A **331**, 211 (1988); U. Hartmann, E. Klempt, and J. Körner, *ibid.* **331**, 217 (1988).
[23] E. Eisenhandler *et al.,* Nucl. Phys. **B96**, 109 (1975).
[24] T. Tanimori *et al.,* Phys. Rev. Lett. **55**, 1835 (1985).
[25] G. Q. Liu and F. Tabakin, Phys. Rev. C **41**, 665 (1990).
[26] M. Kohno and W. Weise, Nucl. Phys. **A454**, 429 (1986).
[27] M. Kohno and W. Weise, Phys. Lett. B **179**, 15 (1986); **206**, 584 (1988); Nucl. Phys. **A479**, 443c (1988).
[28] R. Birsa *et al.,* Nucl. Phys. B (Proc. Suppl.) **8**, 141 (1989); F. Tessarotto *et al.,* in *Proceedings of the 1st Biennial Conference on Low Energy Antiproton Physics, Stockholm, 1990,* edited by P. Carlson, A. Kerek, and S. Szilagyi (World Scientific, Singapore, 1991).
[29] C. Adiels *et al.,* Z. Phys. C **35**, 15 (1987); **42**, 49 (1989).
[30] C. Baltay *et al.,* Phys. Rev. Lett. **15**, 532 (1965); C. Baltay, P. Franzini, G. Lütjens, J. C. Severiens, D. Tycko, and D. Zanello, Phys. Rev. **145**, 1103 (1966).
[31] G. Backenstoss *et al.,* Nucl. Phys. **B228**, 424 (1983).
[32] N. Barash, L. Kirsch, D. Miller, and T. H. Tan, Phys. Rev. **145**, 1095 (1966).
[33] M. Chiba *et al.,* Phys. Rev. D **36**, 3321 (1987); **38**, 2021 (1988); **39**, 3227 (1989).
[34] S. Devons *et al.,* Phys. Rev. Lett. **27**, 1614 (1971).
[35] G. A. Smith, in *Workshop on The Elementary Structure of Matter, Les Houches,* edited by J. M. Richard *et al.,* Springer Proc. Phys. Vol. 26, 1988 (Springer, Berlin, 1988).
[36] C. Amsler, Nucl. Phys. **A508**, 501c (1990).
[37] F. Sai, S. Sakamoto, and S. S. Yamamoto, Nucl. Phys. **B213**, 371 (1983); S. Sakamoto, Y. Kubota, F. Sai, and S. S. Yamamoto, *ibid.* **A412**, 373 (1984).
[38] G. Bardin *et al.,* Phys. Lett. B **192**, 471 (1987).
[39] R. Bizzarri, P. Guidoni, F. Marzano, P. Rossi, D. Zannello, E. Castelli, and M. Sessa, Lett. Nuovo Cimento **1**, 749 (1969).
[40] M. A. Mandelkern, R. R. Burns, P. E. Condon, and J. Schultz, Phys. Rev. D **4**, 2658 (1971).
[41] Y. Sugimoto *et al.,* Phys. Rev. D **37**, 583 (1988).
[42] A. M. Cooper *et al.,* Nucl. Phys. **B146**, 1 (1978).
[43] S. N. Ganguli *et al.,* Nucl. Phys. **B183**, 295 (1981).